AMJ Australasian Medical Journal

[AMJ 2017;10(9):752-758]

Salivary glands scintigraphy with partial volume effects quantification: A phantom feasibility study

Mpumelelo Nyathi[1], Mpho Enoch Sithole[2]

1. Department of Medical Physics, Sefako Makgatho Health Sciences University, South Africa
2. Department of Physics, Sefako Makgatho Health Sciences University, South Africa

RESEARCH

Please cite this paper as: Nyathi M, Sithole ME. Salivary gland scintigraphy with partial volume effects quantification: A phantom feasibility study. AMJ 2017;10(9):752–758.
https://doi.org/10.21767/AMJ.2017.3056

Corresponding Author:
Mpumelelo Nyathi
Department of Medical Physics
Sefako Makgatho Health Sciences University, South Africa
Email: mpumelelo.nyathi@smu.ac.za

ABSTRACT

Background
Salivary gland scintigraphy gives functional information on irradiated glands. Upon irradiation, their size may become less than 2–3 times the resolution of the gamma camera hence underestimation of the regional distribution of administered activity due to partial volume effects (PVEs) which hinder accurate quantification of their function.

Aim
To accurately quantify planar images of spheres mimicking irradiated parotid and submandibular glands with view of implementing salivary gland scintigraphy that involves quantification of PVEs.

Methods
A hollow head and neck phantom was fitted with spheres (diameters: 20mm; 14mm; 12mm and 10mm) filled with technetium-99m solution of activity concentration of 300kBq/mL. The spheres mimicked irradiated parotid glands (right (RP) and left (LP)) and submandibular glands (right (RSM) and left (LSM)) respectively. The phantom was filled with technetium-99m solution of activity concentration 144kBq/mL.[1] A planar image was acquired in 5 minutes using Siemens E-Cam dual head gamma camera detector positioned 5cm vertically above the phantom, on 128×128 matrix size following a thyroid protocol. The detector was fitted with low energy high resolution collimators. ImageJ software was used for quantification.

Results
The image counts post PVEs quantification were: LP=252,213; LP=160,870; RSM=149,072; LSM=68,244. The percentage quantification errors were: 44 per cent, 48 per cent, 51 per cent and 75 per cent for the LP, RP, RSM and LSM glands respectively.

Conclusion
ImageJ software improved quantitative accuracy of sphere images hence it provides a robust quantification tool for irradiated salivary glands.

Key Words
Salivary gland scintigraphy, quantification, partial volume effects

What this study adds:

1. What is known about this subject?
Activity counts or image counts extracted from images of the major pairs of the salivary glands equate to their function.

2. What new information is offered in this study?
Salivary gland scintigraphy can be perfected through quantification of PVEs using ImageJ software. Ability to quantify PVEs leads to accurate measurement of the function of the salivary glands.

3. What are the implications for research, policy, or practice?
Accurate measurement of the function of the diseased or irradiated salivary glands can be achieved through

quantification of PVEs using ImageJ software which is licence free.

Background

Salivary gland imaging plays a significant role in investigating and evaluating the function of diseased salivary glands,[1,2] and irradiated salivary glands.[3-6] Among the common diseases that affect salivary gland function is Sjo¨gren's syndrome (SS). The common clinical symptom of SS and other anomalies affecting salivary glands is usually xerostomia.[3] Xerostomia has been known to result in sticky saliva and nutritional problems.[3-6] Salivary gland scintigraphy (SGS) offers a non-invasive tool for measuring xerostomia.[2-6]

Xerostomia has also been found to be prevalent in other clinical situations such as radiation therapy of head and neck tumours and radioiodine treatment of thyroid cancer.[3,7,8] During therapy of the head and the neck tumours, the parotid glands are affected most because the tumour and lymph nodes are usually found in close proximity to the glands.[3,4] Administration of ionizing radiation in the head and neck regions is associated with acute side effects related to the salivary glands, oral mucosa, mandible and skin.[9,10] However, the loss of salivary glands function is not life threatening.[3,6]

Salivary glands toxicity and accompanying side effects following irradiation degrade the quality of life of patients treated for head and neck tumours. In addition to xerostomia, patients treated for head and neck tumours suffer from speech problems, oral infections and dental curies.[10-15] In order to improve the quality of life of people previously treated for head and neck tumours, clinicians and researchers need detailed knowledge about the side effects of radiation therapy. This information is acquired through imaging of salivary glands during the course of therapy or post-therapy. Salivary gland scintigraphy is one of the techniques used to evaluate functional information needed for implementation of effective patient management schemes.

One of the main advantages of salivary gland scintigraphy (SGS),[9-11] over other imaging modalities (Magnetic Resonance Imaging (MRI), Computed Tomography (CT), Ultrasound (US), Sialography, Magnetic Resonance Sialography (MR-Sialography)[11-15] is that it has the ability to offer functional information compared to structural and anatomical information derived from the modalities mentioned above. Currently, SGS is used at qualitative and semi-quantitative levels to evaluate salivary gland function as well as to examine parenchymal impairment.[2-8]

The qualitative techniques rely on activity uptake by individual glands pre and post-therapy which are used to draw activity-time graphs for each individual gland. The function is then inferred from the activity-time graphs.[2,6] The semi-quantitative methods are based on activity uptake and washout fraction. The uptake rate of the activity (radiotracer) by individual gland is expressed as count rate per second (cps/s). The latter are obtained from regions of interests drawn on dynamic images of individual parotid and submandibular glands.[2,6,16] However, both qualitative and semi-quantitative methods despite their ability to offer functional information lack accuracy due to underestimation of the regional distribution of activity in the glands caused by the limited spatial resolution of the gamma camera imaging system.

Salivary glands upon irradiation loss acinar cells,[10] their size shrinks resulting in their diameters approximating 2-3 times the resolution of the gamma camera. They therefore become prone to PVEs hence quantitative errors in salivary gland scintigraphy.

The PVEs may manifest either as spill-out effects or spill-in effects. The spill-out effects are a result of "loss" of activity from the organ of interest into the background resulting in underestimation of the regional distribution of organ activity. The spill-in effects occur when activity from the neighbouring structure or background blurs into organ of interest leading to overestimation of the detected nuclear medicine signal.[1,17-19]

Both effects, the spill-out and spill-in occur simultaneously in a radioactive background resulting in cancellation of some spill-out and spill-in activity counts thereby reducing quantitative errors associated with PVEs.[1,17-19] However, in the absence of a radioactive background only the spill-out effects occur.[1]

In quantitative SPECT studies, PVEs have been found to cause shape distortions that are dependent on activity distribution in the targeted structures as well as in the surrounding structures.[18,19] According to Rousset et al.,[18] PVEs may change both the magnitude and shape of the time-activity curves introducing an error of 50 per cent in the estimated count rates per second for metabolism and transfer of activity between compartments of the human brain. Similarly, we would expect the shapes of the individual submandibular and parotid glands' activity-time curves used to infer function to be besieged by errors of the

same magnitude or slightly less thus rendering functional information deduced from curves inaccurate. In order to achieve accuracy, technetium-99m activity counts spread due to PVEs should be quantified before generating the activity-time curves for each individual gland that are used to infer on their function.

In order to achieve accurate quantitative results in tomographic imaging, it has since been agreed in principle that the limitations associated with the PVEs that need to be resolved.[17,19-27] Many techniques for PVEs correction have since been proposed.[19,22-24,27] Ritt et al.,[28] divided the PVEs correction techniques into two groups. The first group requires additional anatomical information on imaged structures in order to effect PVEs correction. Anatomical information may be acquired using either CT or MRI modality. The second group relies solely on emission images and encompasses post re-construction approach. Nyathi et al.,[29] latter proposed use of ImageJ software, a licence software for PVEs quantification. However, the technique requires the knowledge of the spatial resolution of the gamma camera. The technique relies on two regions of interest (ROIs). ROI 1 firmly touches the boundary of the image while ROI 2 extends from ROI 1 by the full width half maximum (FWHM) of the gamma camera. ROI 2 recovers image counts spread to the neighboring image pixels as a result of PVEs. Use of ImageJ is cost effective unlike use of CT or MRI which may not be available in economically strained departments.

In salivary gland scintigraphy, quantitative accuracy is hindered by failure to account for the activity counts spread due to PVEs. In order to overcome this limitation, this study proposes quantification of PVEs in salivary gland scintigraphy. The aim of this study was to accurately quantify planar images of spheres mimicking irradiated parotid and submandibular glands with the view of implementing salivary gland scintigraphy that involves quantification of PVEs.

Materials and Methods

Phantom preparation

A hollow head and neck phantom shown in Figure 1 was fitted with spheres (diameters: 20mm; 14mm; 12mm and 10 mm) filled with technetium-99m solution of an activity concentration of 300kBq/mL. The spheres mimicked irradiated parotid glands (right (RP) and left (LP)) and submandibular glands (right (RSM) and left (LSM)) respectively.

The following assumptions were made about the salivary glands:

1. The volume of RP, the right parotid gland was bigger in comparison to the left parotid gland named as LP. The volume of RP was assumed to approximate to that of a healthy person with no radiation injuries. Under normal circumstances the two glands should have had the same size. However, due to radiation injury, the LP gland lost some of its acinar cells hence reduction in its volume.
2. The volume of the RMS was assumed to be intact hence it was bigger than that of LSM which was assumed to have been severely injured during therapy. RSM resembled a healthy submandibular gland.

The spheres (salivary glands) were firmly fixed inside the head and neck phantom using wax in positions of the parotid and submandibular glands in normal humans. The wax kept them in fixed positions throughout imaging. The head and neck phantom was filled with technetium-99m solution of an activity concentration of 144kBq/mL to provide background activity thus resembling a clinical scenario in which activity exists in the blood pool proving background radiation. This background activity was found to effectively reduce the impact of spill-out and spill-in effects as some activity counts associated with these two effects tended to cancel each other thus reducing quantification errors due to partial volume effects.[1] Spill-in effects resulted in movement of the activity counts from the background technetium-99m solution filled into the head and neck phantom into the peripheral boundaries of the four glands resulting in overestimation of image counts. On the other hand spill-out effects resulted in movement of the activity counts from the individual glands to the background resulting in apparent loss of activity inside each individual gland. However, cancellation of activity counts attributed to the two effects resulted in reduction of the impact of PVEs.

Imaging technique

The head and neck phantom was imaged while placed on supine position on the imaging table using one detector of a Siemens E-Cam dual head gamma camera placed 5cm vertically above the phantom (Figure 1). A thyroid protocol was used. The detector was fitted with low energy high resolution (LEHR) collimators. The planar image was acquired on a matrix size of 128×128 pixels in a period that lasted 5 minutes.

Image quantification

Three duplicates of the planar image of the head and neck phantom were copied from the processing station into a

personal laptop installed with ImageJ software [version 1.48a; Java 1.70_51 [64-bit]. All the three images were quantified using ROI 1 and ROI 2 inserted using the circular tool of ImageJ software following the method proposed by Nyathi et al.,[29] (Figure 2). ROI 2 extended from the boundary of ROI 1 by the FWHM of the gamma camera (4.5mm), a value measured at a distance of 5cm from the point source.[1] Quantification was repeated three times on each gland and the mean value was calculated (Table 1).

Results and Discussion

Table 1 shows images counts extracted from the images of the RP, LP, RSM and LSM glands. The phantom image was duplicated to facilitate three measurements on each gland during quantification. Columns 2; 3 and 4 gives image counts of each individual gland obtained using ROI 1, these exclude image counts spread by the PVEs. Column 5 shows the mean measurement for each gland.

Column 6; 7 and 8 show image counts extracted using ROI 2 from each individual gland. These counts include image counts that were spread to the neighbouring pixels due to PVEs. The image counts presented in column 9 are the mean values for each gland extracted post PVEs quantification. Column 10 shows the actual image counts that were spread by the PVEs also referred to as "recovered image counts" in Table 1. These image counts were obtained by subtracting the mean value of ROI 1 from the mean values of ROI 2 for each gland. The recovered image counts were found substantial for each gland thus making PVEs quantification mandatory in quantitative planar imaging.

The percentage error in Table 1 was calculated using the formula:

$$\%\,\text{Error} = \frac{\text{Recovered Image Counts}}{\text{Image Counts extracted post PVEs quantifification}} \times 100 \quad [1]$$

Classification of the level of damage of the parotid and the submandibular glands

The 252,213 image counts extracted from the RP corresponded to those that would have been extracted from an intact gland pre radiation therapy. In patient studies, it is recommended that the salivary glands be imaged pre and post therapy. The image counts registered pre therapy must be compared to those registered post therapies so as to differentiate between their function pre and post therapy. However, should absolute quantification be required then image counts should be converted to activity concentration.

The sizes of the glands were varied in order to accommodate changes in size and function of the gland as a result of radiation injury. The lesser the measured counts the more damage on the particular gland. A total of 149,072 image counts were extracted from the RSM, this gland was assumed to be intact. It represented a RSM that has not been irradiated. These image counts saved as a baseline indicator of a non-irradiated submandibular gland. Image counts below this value suggest that damage has been inflicted by ionizing radiation during therapy.

Interpretation of results

The study results (Table 1) revealed the challenges of accurate quantification of the image counts from the images of the salivary glands post therapy. From the findings presented in column 8, it became apparently clear that PVEs indeed hinder accurate quantification. The presence of PVEs is attributed to the limited spatial resolution of the gamma camera that caused the image counts to spread out. At first attempt, the quantification procedure failed to recover the image counts that were spread out (Table 1, column 5). The spread of these imaged counts was due to apparent loss of technetium-99m activity counts from the RP, LP, LSM and RSM. However, use of ImageJ facilitated recovery of the "lost" image counts and ultimate accurate quantification of images of the individual glands (Table 1, column 9).

A comparison of image counts corresponding to each individual gland pre and post PVEs quantification showed a huge difference. The images counts pre quantification of PVEs corresponding to the RP, LP, RSM and LSM were: 141,573; 89,995; 73,900 and 17,007 respectively compared to 252,213; 160,870; 149,072 and 68,244 respectively post PVEs for the same glands. These values may have been overestimated due the presence of a radioactive background However, this was ignored because a study by Nyathi,[1] established that the spill-in effects and the spill-out effects cancel each other when a background of 144kBq/mL was used when the structures were filled with technetium-99 solution of activity concentration of 300kBq/mL.

From the study, it was also found that the quantification error increased with decrease in the size of the gland. The smallest LSM gland registered a quantification error of 75 per cent compared to of 44 per cent for the largest RP gland. The margin of the quantification errors established in this study lead to a conclusion that quantification of PVEs should be prioritised during quantitative evaluation of the parotid and submandibular glands post radiation therapy. Quantification of PVEs was found to be worsened by the dramatic decrease in the sphere size. The salivary glands

lose acinar cells as a result of radiation injury hence reduction in volume. The reduction in size makes them susceptible to PVEs by virtue of their size in comparison to the dimensions of the resolution of the gamma camera.

From Table 1, it was also observed that the percentage quantification error for the glands (RP, LP, RSM and LSM) were 44 per cent, 48 per cent, 51 per cent and 75 per cent respectively. However, use of ImageJ software facilitated accurate quantification of the salivary glands. The function of each individual gland was therefore inferred from its image counts. The lesser the image counts registered, the more damage was inflicted during therapy. The quantification based on image counts is relative. In clinical studies it would be helpful if absolute quantification is calculated. In that case it would be important to measure the gamma camera sensitivity which is required when converting image counts into activity concentration.

Conclusion

SGS is a reproducible, sensitive tool for monitoring salivary gland dysfunction due diseases and radiation injury. However, PVEs quantification remains as a pre-requisite for accurate quantification of image counts. The function is equated image counts.

References

1. Nyathi M. Quantitative evaluation of the parotid and submandibular glands post radiation therapy of head and neck tumours. PhD thesis. Sefako Makgatho Health Sciences University. Ga-Rankuwa. South Africa. 2015.
2. Henriksen AN, Nossent HC. Quantitative salivary gland scintigraphy can distinguish patients with primary Sjøgren's syndrome during the evaluation of sicca symptoms. Clin Rheumatol. 2007;26:1837–1841.
3. Loutfi I, Nair MK, Ebrahim AK. Salivary Gland Scintigraphy: The Use of Semi quantitative Analysis for Uptake and Clearance. J Nucl Med Technol. 2003;31:81–85.
4. Munter MW, Karger CP, Hoffener SG, et al. Evaluation of the salivary gland function after treatment of head-and-neck tumours with intensity modulated radiotherapy by quantitative pertechnetate scintigraphy. Int J Radiat Oncol Biol Phys. 2004;58(1):175–184.
5. Braam P. Parotid gland sparing radiotherapy. Utrecht, The Netherlands, Elsevier Science Inc; 2007.
6. Valdez IH. Radiation-induced salivary dysfunction: clinical course and significance. Spec Care Dentist. 1991;11:252–255.
7. Solans R, Bosch JA, Galofre P, et al. Salivary and lacrimal gland dysfunction (sicca syndrome) after radioiodine therapy. J Nucl Med. 2001;42:738–743.
8. Liem IH, Olmos RA, Balm AJ, et al. Evidence for early and persistent impairment of salivary gland excretion after irradiation of head and neck tumours. Eur J Nucl Med. 1996;23:1485–1490.
9. Head and Neck Cancers. National Institute of Cancer. [Internet]. 2017 [cited 2017 Apr 10]. Available from: http://www.cancer.gov/cancertopics/types/head-and-neck.
10. Cheng SC, WU VWC, Kwong DLW, et al. Assessment of post-radiotherapy salivary gland. Brit J Radiol. 2011;84:393–402.
11. Nishimura Y, Nakamatsu K, Shibata T, et al. Importance of the initial volume of Parotid Glands in Xerostomia for patients with neck tumours treated with IMRT. Jpn J Oncology. 2005;35:375–379.
12. Vissink A, Jansma J, Spijkervet FKL, et al. Oral Sequelae of head and neck radiotherapy. Crit Rev Oral Biol M. 2003;14:199–212.
13. Jimenez-Heffernan A, Gomez M, Sanchez De Mora E, et al. Quantitative salivary gland scintigraphy in the head and neck cancer patients following radiotherapy. Rev Esp Med Nucl. 2010;29:165–171.
14. Cheng VST, Downs J, Aramny M. The function of the parotid gland following radiotherapy for the head and neck cancer. Int J Radiat Oncol. 1981;7:253–258.
15. Parliament M, Scrimger R, Anderson R, et al. Oral-related quality of life preserved after inverse-planned intensity modulated radiotherapy (IMRT) for head and neck cancer (HNC). CRO 2002-Innovative Technology in Radiation Medicine. 25-27 October 2002.
16. Klutmann S, Bohuslavizki KH, Kroger S, et al. Quantitative Salivary Gland Scintigraphy. J Nucl Med Technol. 1999;27:20–26.
17. Hoettjes NJ, van Velden FHP, Hoekstra OS, et al. Partial volume correction strategies for quantitative FDG in oncology. Eur J Nucl Med Mol Imaging. 2010;37(9):1679–1687.
18. Rousset OG, Ma Y, Evans AC. Correction for partial volume effects in PET: principle and validation. J Nucl Med. 1998;39:904–911.
19. Erlandsson K, Buvat I, Hendrik Pretorius PH, et al. A review of partial volume correction techniques for emission tomography and their applications in neurology, cardiology and oncology. Phys Med Biol. 2012;57:R119–R159.
20. Buvat I. Quantification in emission tomography: challenges, solution, and performance. Nucl Instrum Meth A. 2007;571:10–13.

21. Hofheinz F, Dittrich S, Potzsch C, et al. Effects of cold sphere walls in PET measurements on the volume reproducing threshold. Phys Med Biol. 2010;55:1099–1113.
22. Kirov AS, Pia JZ, Scmidtlein CR. Partial volume correction in PET using iterative deconvolution with variance control based on local topology. [Internet] 2015. [cited 2015 Dec 1]. Available from: http://www.iop.orgEJ/abstract/0031-9155/53/10/009.
23. Rabilotta CC. Emission tomography: SPECT and PET. Computation and systems. 2004:167–174.
24. Teo BK, Seo Y, Bacharach SL, et al. Franc BL. Partial Volume correction in PET: Validation of an Iterative Post reconstruction Method with Phantom and Patient Studies. J Nucl Med. 2007;48:802–810.
25. Strul D, Berndriem B. Robustness of Anatomically Guided Pixel-by-Pixel Algorithms for Partial Volume Effect Correction in Cereb Blood Flow Metab. 1999;19:547–559.
26. Soret M, Bacharach SL, Buvat I. Partial Volume Effect in PET Tumour Imaging. J Nucl Med. 2007;48:932–945.
27. Buvat I. Partial volume effect issue: Instrumental and biological components. Taormina workshop. 2012; Aug 31; Orsay, France.
28. Ritt P, Vija H, Hornegger J, et al. Absolute quantification in SPECT. Eur J Nucl Mol Imaging. 2011;38:S69–S77.
29. Nyathi M, Sithole ME, Ramafi OE. Quantification of Partial Volume effects in Planar Imaging. Iran J Nucl. 2016;24(2):116–120.

ACKNOWLEDGEMENTS

The authors would like to acknowledge the Department of Nuclear Medicine at Dr George Mukhari Academic Hospital for availing the premises and the Siemens E-Cam dual head gamma camera used in this study.

PEER REVIEW

Not commissioned. Externally peer reviewed.

CONFLICTS OF INTEREST

The authors declare that they have no competing interests.

FUNDING

None

ETHICS COMMITTEE APPROVAL

This study was approved by the research committee of the Medunsa Campus of University of Limpopo, now Sefako Makgatho Health Sciences University under the clearance number: REC/P/280/2012: PG

Figure 1: Head and neck torso placed on a supine position on the imaging table below the detector head #1 of a Siemens E-Cam dual head gamma camera

Figure 2: ROI 1 and ROI 2 drawn on individual parotid and the submandibular glands

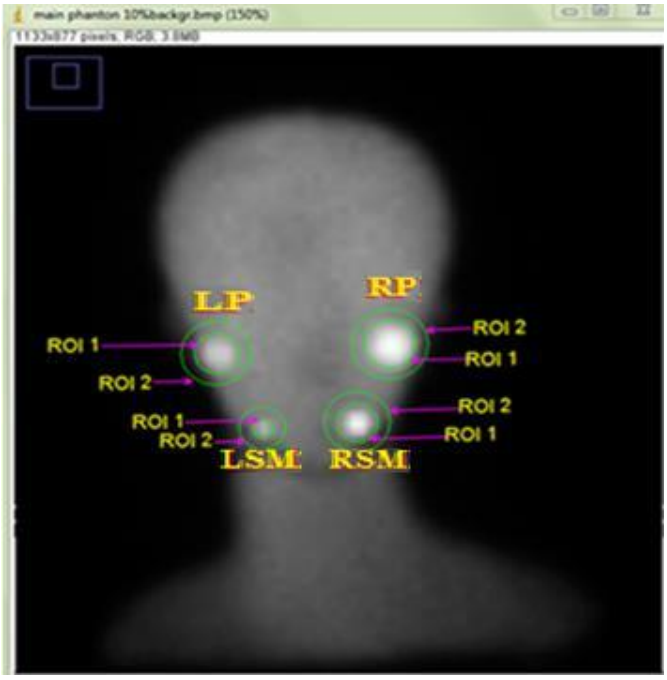

Table 1: Image counts extracted from parotid and submandibular glands before and after PVEs quantification

Name of Salivary gland	ROI 1 Image counts before PVEs quantification				ROI 2 Image counts after PVEs quantification				Recovered image counts	Quantification Error	Level of radiation damage
	Measurements				Measurements				Measurements	%	Grade
	1	2	3	$\overline{ROI\ 1}$	1	2	3	$\overline{ROI\ 2}$	$\overline{ROI\ 2} - \overline{ROI1}$	% Error	Intact/Moderate/Severe
RP	142,000	142,445	141,145	141,l573	251,950	252,690	252,000	252,213	110,640	44	Intact
LP	84,000	84,259	83,990	83,995	160,690	160,836	161,050	160,870	76,875	48	Moderate
RSM	73,780	73,820	74,100	73,900	148,900	149,315	149,000	149,072	75,172	50	Intact
LSM	17,000	17,041	16,980	17,007	68,340	68,292	68,100	68,244	51,237	75	Severe